Received: 29 March 2025 | Revised: 8 September 2025 | Accepted: 17 December 2025 | Published online: 12 January 2026

RESEARCH ARTICLE

Journal of Optics and Photonics Research
2026, Vol. 00(00) 1–8
DOI: 10.47852/bonviewJOPR62025710

BON VIEW PUBLISHING

Comparative Analysis of Corneal and Lens Doses in Nuclear Medicine and Impact of Lead Eyeglasses: A Monte Carlo Simulation Approach

Zahra Akbari Khanaposhtani[1] and Hossein Rajabi[1,*]

[1] *Department of Medical Physics, Tarbiat Modares University, Iran*

Abstract: Research on eye lens dosimetry for radiation workers has increased after the 2012 International Commission on Radiological Protection 118 update on eye lens dose limits, while corneal dosimetry has remained underexplored due to historical focus and measurement challenges. This study employed a high-resolution digital eye phantom in Monte Carlo simulations to estimate corneal and lens doses for nuclear medicine staff, with and without lead glasses. Using the Monte Carlo code GATE (Geant4 Application for Tomographic Emission) (version 9.0), based on the GEANT4 toolkit (version 10.6), we estimated doses from primary and scattered radiation emitted by common radionuclides (F^{18}, I^{131}, Tc^{99m}) under varying lead glass shielding thicknesses (0–0.75 mm). The simulations demonstrated that across all radionuclides, the dose to the cornea was consistently higher than the dose to the lens. Moreover, the ratio of corneal to lens dose increased with thicker lead glasses, reflecting a greater relative dose reduction to the lens. These findings indicate that while thicker lead glasses enhance lens protection, they reduce corneal exposure less effectively, thereby raising the cornea-to-lens dose ratio. Although protective eyewear remains important, its practicality may be limited by diminishing returns in shielding effectiveness and potential discomfort. Overall, this work highlights the necessity of considering both corneal and lens dosimetry to optimize occupational eye protection strategies in nuclear medicine.

Keywords: corneal dosimetry, lens dosimetry, Monte Carlo, GATE, nuclear medicine, simulation

1. Introduction

Radiation workers, including nuclear medicine personnel and interventional radiologists, are routinely exposed to ionizing radiation such as gamma rays and X-rays [1]. In nuclear medicine, professionals often handle unsealed radionuclide sources, leading to localized exposure, particularly to the extremities, but ocular exposure has emerged as an increasingly important concern [2]. Adherence to safety protocols and the use of advanced shielding techniques remain essential for minimizing risks in these high-exposure environments.

The eye is one of the most radiosensitive organs, with the lens particularly vulnerable to ionizing radiation. Cataract formation, classified as a deterministic effect, occurs when dose thresholds are exceeded. Historically, radiation-induced cataracts were believed to develop only above 2 Gy, but subsequent studies revealed that lens opacities may appear at substantially lower doses [3]. This evidence prompted the International Commission on Radiological Protection (ICRP) to revise its recommendations in Publication 118, lowering the threshold to 0.5 Gy for chronic exposure [4]. Consequently, the occupational dose limit for the lens was reduced to 20 mSv per year, averaged over five years, with no single year exceeding 50 mSv [4]. These changes reflect the growing recognition of the eye's radiosensitivity and the need for stringent safety standards [5].

Cataracts remain the most common radiation-related ocular complication, associated with glare, halos, and impaired night vision. Surgical replacement of the lens with a synthetic intraocular lens remains the gold standard for restoring functional vision. While effective, surgery has limitations, and research is increasingly focused on pharmaceutical and noninvasive strategies to delay cataract progression or improve accessibility to care [6].

In addition to cataracts, other ocular tissues such as the cornea are also at risk. Although the cornea has historically received less attention than the lens, emerging evidence indicates that surface interactions with radiation can produce measurable absorbed doses [7]. Low-energy photons and secondary electrons generated in the surrounding environment can deposit dose at the corneal surface [7]. While such exposures are generally not linked to deterministic effects at low doses, they may become relevant in high-dose or high-frequency clinical settings. Understanding corneal dose, in addition to lens dose, is therefore important for comprehensive ocular protection.

International guidelines now emphasize accurate dosimetry and the application of operational quantities such as Hp(3) for eye dose monitoring [4]. Numerous studies have confirmed that occupational doses in nuclear medicine and interventional radiology can approach or even exceed regulatory limits, highlighting the importance of monitoring and protective eyewear [8, 9]. A recent multicenter survey further confirmed considerable variability in

***Corresponding author:** Hossein Rajabi, Department of Medical Physics, Tarbiat Modares University, Iran. Email: hrajabi@modares.ac.ir

occupational eye lens doses across nuclear medicine departments [8, 9]. For instance, Bellamy et al. [8] demonstrated consistent occupational exposure to the eye lens among staff in high-volume centers, showing that technologists working near unsealed sources may exceed annual dose constraints without proper shielding. More recent simulation-based studies confirm that protective eyewear can significantly reduce ocular doses, though the effectiveness varies with design and angular dependence [10, 11].

Recent research has also highlighted differences between absorbed dose and equivalent dose for ocular assessments. While equivalent dose (measured in Sievert) accounts for radiation type through a weighting factor, absorbed dose (measured in Gray) is considered more appropriate for deterministic effects such as cataracts [4]. This distinction reinforces the importance of accurate measurement methods and simulation tools for risk estimation.

Monte Carlo simulations have become a key approach for assessing eye lens and corneal doses in both clinical and research contexts [12]. These simulations enable detailed modeling of radiation interactions in ocular structures under different protective conditions [13]. For example, Morhrasi et al. [2] and Hoeijmakers et al. [13] demonstrated how varying eyewear thickness and geometry affect the absorbed dose distribution. Similarly, recent studies in nuclear medicine staff show that lens doses remain **below** the new occupational limit (20 mSv/year) when optimized shielding and protective equipment are used [8, 9].

The role of the cornea is particularly relevant in dosimetry, as it is the first ocular tissue encountered by radiation. Recent studies have emphasized the potential for corneal dose accumulation in certain scenarios, particularly where low-energy radiation predominates [7]. Nuzzi et al. [14] reported that while radiation-related corneal injury is rare, the risk cannot be ignored, particularly in therapeutic exposures. Although most keratitis cases are linked to ultraviolet exposure**,** ionizing radiation following radiotherapy has also been implicated in rare cases [14]. This supports the value of corneal dose monitoring as a complementary metric for ocular-risk assessment in high-risk workplaces [7, 12].

Protective strategies must therefore address both lens and cornea. Recent investigations into radiation-protective eyewear have shown that lead glasses can effectively reduce absorbed doses, though their efficiency is influenced by angle of exposure and design [10, 11]. Akahane et al. [15] confirmed variations in attenuation performance across different protective eyewear types, and Hirata et al. [16] demonstrated that angular dependence is a critical factor in determining overall protection. These findings indicate that protective equipment must be carefully selected to achieve meaningful dose reduction.

This study aims to evaluate the radiation dose distributions to both the cornea and lens using Monte Carlo simulations of photon emissions from radionuclides commonly used in nuclear medicine, as well as X-rays applied in interventional radiology. Scenarios with and without protective eyewear of varying thicknesses were modeled. The resulting data provide a comparative assessment of ocular radiation exposure, with the goal of informing improved protective strategies for medical staff routinely exposed to ionizing radiation.

2. Methods and Materials

2.1. Monte Carlo simulation

Geant4 Application for Tomographic Emission (GATE) (version 9.0) was employed to calculate absorbed doses in the study geometry [17]. Built on the Geometry and Tracking 4 (GEANT4) (version 10.6), GATE is a Monte Carlo toolkit tailored for nuclear medicine [18]. It models photon and electron interactions, including photoelectric absorption, scattering, ionization, X-ray production, and Auger emission.

Among four available physics models, the Livermore model was chosen for its accuracy in simulating low-energy electromagnetic interactions critical for ocular dosimetry. Recent validation studies using similar Monte Carlo approaches have confirmed the accuracy of such low-energy interaction modeling for ocular dose estimation [13]. It tracks particles down to 250 eV, ensuring precise simulation of low-energy contributions to eye dose [12]. Based on EPDL97, EEDL, and EADL libraries, the Livermore model provides reliable tissue-level interaction data, with sub-threshold energy deposited locally.

A step size of 0.01 mm was applied, and 200 million histories were simulated, maintaining cornea and lens dose uncertainties below 0.01. Doses were normalized per MBq·s (1 MBq for one second, i.e., one million decays), aligning outputs with clinical activity-based references and ensuring robust dosimetric evaluation.

2.2. Geometry of simulation

A three-dimensional (3D) ocular model in OBJ format, developed by Wavefront Technologies [19], was used. The half-eye model was processed with Binvox software (Min, 2004–2021, available at http://www.patrickmin.com/binvox) to generate a voxelized 3D phantom with a resolution of 0.039 × 0.046 × 0.097 mm. Only the cornea, lens, and related tissues were included, and MATLAB scripts distinguished their regions MATLAB R2023a (The MathWorks Inc., Natick, MA, USA). Tissue composition was derived from the ICRP reference values for eye tissues (ICRP Publication 89). These values are summarized in Table 1.

Protective lead glasses were modeled as a 30 × 30 × X mm box 9 mm from the eye, matching typical clinical geometry. The simulation included forward scattering of secondary electrons from photoelectric and Compton interactions. Lead-glass shielding was modeled with thicknesses ranging from 0 to 0.75 mm and a density

Table 1
Atomic composition (by weight fraction) of different tissues of the eye used in the simulation

	Weight Fraction (%)									
Tissue	H	C	N	O	Na	P	S	Cl	K	Ar
Lens	0.096	0.195	0.057	0.646	0.001	0.001	0.003	0.001	–	–
Eyeball	0.107	0.069	0.017	0.803	–	0.001	0.001	–	–	0.002
Cornea*	0.102	0.143	0.034	0.708	0.002	0.003	0.003	0.002	0.003	–

Note: *The ICRU-recommended eye soft tissue was used as a proxy for the cornea tissue.

Figure 1
The schematic representation of geometry used in this study

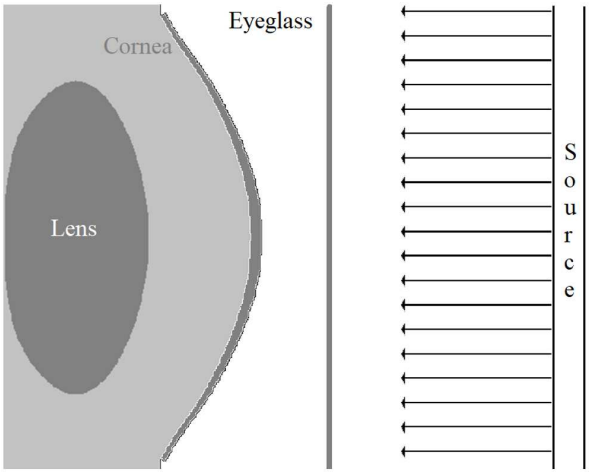

of 11.4 g/cm³, representative of pure lead. In practice, commercial protective eyewear often uses lead-oxide glass with slightly lower effective density. Using pure-lead density ensured consistency with prior models. Zero thickness indicated no protection. Figure 1 shows the geometry.

The voxelized model, though simplified, captures key ocular structures for dose assessment. Unlike the more detailed Behrens model [12]. It favors computational efficiency for large-scale Monte Carlo runs. Despite simplification, corneal and lens volumes remain within accepted anatomical limits, supporting valid comparative dosimetry. Future work could implement refined geometries to improve spatial and dosimetric accuracy for smaller ocular regions.

2.3. Spectra of radiation

In this study, three commonly used radionuclides in nuclear medicine—fluorine-18 (F^{18}), technetium-99m (Tc^{99m}), and iodine-131 (I^{131})—were selected to evaluate the absorbed dose to the cornea and lens. These isotopes represent a range of photon energies (140 keV for Tc-99m, 511 keV for F-18, and 364 keV for I-131), enabling comprehensive assessment across diagnostic and therapeutic energy levels [20]. The radionuclide emission spectra I^{131}, Tc^{99m}, and F^{18} were taken from standard Medical Internal Radiation Dose (MIRD) radionuclide data tables commonly used in nuclear medicine dosimetry [20]. For this study, only the X-ray and gamma radiation spectra were utilized, as other forms of radiation are negligible at a distance from the radionuclide source. These spectra simulated radiation exposure in a controlled hot laboratory environment.

Additionally, two X-ray spectra with peak energies of 30 and 50 keV were included to represent scattered radiation typically encountered in interventional radiology procedures. These energy levels were selected to represent the most probable scatter photon energies reaching eye level during fluoroscopic procedures, particularly in cardiac and other interventional radiology applications where soft X-rays are prevalent and lead eye protection demonstrates its greatest effectiveness [21].

This addition allows for comparison between radionuclide-based exposure in nuclear medicine and secondary radiation exposures from X-rays used in interventional settings. The selected spectra help explore how different photon energies interact with ocular tissues and protective eyewear, providing valuable insight into energy-dependent shielding effectiveness and biological dose depositions [10]. This experimental setup allowed for the precise evaluation of radiation interactions while maintaining standardized conditions. However, in real-life clinical settings, technologists often observe the source at a downward angle. This deviation in head orientation could influence the radiation dose received by the eye and may lead to variation in shielding effectiveness [10].

2.4. Estimation of the corneal and lens doses

The energy spectra of radiation generated in the preceding stages were utilized to irradiate an eye phantom. This radiation was applied uniformly and parallel across the entire phantom, with the source designed to encompass the whole cross-sectional area of the eye model. Each simulation generated two binary output files of dimensions comparable to the eye phantom. The first file contained voxel-specific dose data, while the second provided the associated uncertainties for each voxel.

A custom MATLAB script was used to extract dose values and their corresponding uncertainties for the phantom tissues. Despite the large number of voxels analyzed, the maximum statistical uncertainty recorded across all simulation outputs was determined to be 0.01 (1%), which indicates that the relative error in the calculated absorbed dose per voxel is within 1%. In Monte Carlo simulations, this metric reflects the confidence in dose estimation due to the finite number of particle histories used, ensuring high precision and reliability of results.

The values in Table 2 represent dose conversion factors, expressed in mGy per one million incident photons (i.e., per 1 MBq·s assuming one million decays). These values do not reflect absolute clinical dose but instead provide a standardized metric for comparing dose deposition across different scenarios. To express the dose in μGy/MBq, we normalized the results to one disintegration per photon, consistent with the assumption of 1 MBq·s producing one million decays. Although the simulation setup assumes parallel and orthogonal beam geometry, real-life exposure may involve varying incident angles depending on the technologist's position and source geometry. As such, our results represent idealized baseline conditions, which could be expanded upon in future work using more anatomically dynamic models and angular distributions.

3. Result

3.1. Dose to different parts of the eye

Table 2 comprehensively summarizes the radiation dose to various eye components, including the lens, cornea, and total ocular tissues. A pooled dataset encompassing all radionuclides was analyzed using a paired *t*-test to evaluate dose distribution. The analysis revealed no statistically significant differences between the dose to the lens and the overall ocular tissues (p-value < 0.001). Conversely, a significant difference was observed between the dose to the cornea and other ocular tissues (p-value > 0.75).

These findings indicate that the radiation dose to the lens can be considered a reliable representation of the total ocular dose. This conclusion has important implications for simplifying dose assessment protocols in radiological studies, as it underscores the lens as an appropriate surrogate for evaluating overall ocular exposure.

While absolute dose values for radionuclides are provided in Table 2, X-ray simulations were used specifically to evaluate cornea-to-lens dose ratios (Table 3), and thus, their results are not included here due to methodological differences.

Table 2
The doses to the lens, cornea, and eye tissues in mGy per one million photons from the radionuclides

Eye glass (mm)	F^{18}			I^{131}			Tc^{99m}		
	Lens	Cornea	Eye	Lens	Cornea	Eye	Lens	Cornea	Eye
0.0	8.21	9.06	8.39	5.69	6.23	5.82	1.75	2.07	1.82
0.05	8.13	9.01	8.32	5.62	6.16	5.74	1.53	1.83	1.60
0.07	8.11	8.96	8.30	5.59	6.13	5.71	1.45	1.73	1.52
0.10	8.07	8.93	8.26	5.54	6.08	5.66	1.34	1.61	1.41
0.20	7.95	8.79	8.13	5.38	5.92	5.51	1.04	1.24	1.08
0.30	7.82	8.66	8.00	5.24	5.75	5.36	0.80	0.96	0.83
0.40	7.69	8.53	7.88	5.11	5.62	5.22	0.61	0.74	0.64
0.50	7.57	8.45	7.76	4.97	5.48	5.08	0.47	0.57	0.50
0.60	7.45	8.31	7.64	4.84	5.34	4.95	0.36	0.44	0.38
0.70	7.33	8.18	7.52	4.71	5.22	4.82	0.28	0.34	0.29
0.75	7.27	8.10	7.46	4.64	5.14	4.76	0.24	0.30	0.26

3.2. The ratio of cornea-to-lens dose

Table 3 presents the ratio of cornea-to-lens radiation exposure, considering photon energy levels and the thickness of lead glasses used for eye protection. The results indicate an inverse relationship between this ratio and photon energy. Specifically, as the mean photon energy decreases, the cornea-to-lens ratio increases. Understanding the cornea-to-lens dose ratio is important because it reflects how radiation interacts with anterior ocular tissues and helps assess whether shielding strategies designed for the lens also offer protection for the cornea.

The mean photon energies for F^{18}, I^{131}, and Tc^{99m} are approximately 511 keV, 364 keV, and 140 keV, respectively. These values represent the dominant gamma or annihilation photon emissions used in diagnostic or therapeutic procedures. Mean photon energy is used here as a metric to characterize the penetrating ability and interaction probability of each radionuclide with ocular tissues. Higher-energy photons tend to deposit dose deeper in tissue, influencing the dose distribution between the cornea and lens.

Similarly, the cornea-to-lens ratio for beta radiation follows a comparable trend: beta emitters like Tc-99m or Lu-177 deliver relatively higher doses to the cornea than to the lens, as indicated by dose conversion coefficients from recent Monte Carlo and validated experimental work [13].

Furthermore, a positive correlation is observed between the cornea-to-lens ratio and the thickness of lead glasses. Increasing the thickness of lead shielding reduces the absorbed dose to both the cornea and lens, even as the average radiation energy decreases.

For monoenergetic X-ray electrons at 30 keV, the cornea-to-lens ratio is approximately 1.8 times that at 50 keV without shielding. However, as the thickness of lead glass increases, this ratio diminishes significantly. These findings highlight the importance of optimizing lead glass shielding to mitigate radiation exposure effectively while considering photon energy levels.

The X-ray simulations in this study utilized monochromatic photon beams (30 keV and 50 keV) as a simplified approach to explore cornea-to-lens dose ratios. While such simplification aids in isolating the influence of photon energy on dose distribution, it does not fully represent the spectral characteristics of diagnostic or interventional X-ray sources. In clinical practice, occupational eye exposure is predominantly due to scattered radiation with broad spectral distributions, not direct primary beams. Therefore, these results may underestimate the actual protection factors provided by lead eyewear. Future studies will incorporate realistic spectra and scattering conditions to better reflect clinical exposure scenarios.

3.3. Protection efficiency of the lead eyeglasses

Figure 2 illustrates the protection efficiency of lead glasses when exposed to various radionuclides investigated in this study. Protection efficiency is defined as the percentage reduction in radiation dose achieved by wearing the lead glasses compared to no shielding. The results indicate that the protective capability of lead glasses for nuclear medicine personnel is limited. However, this limitation is influenced by the energy of the radiation emitted from different radionuclides. For instance, lead glasses offer greater attenuation for lower-energy photons (e.g., Tc^{99m} at 140 keV) but become less effective for higher-energy emissions like F^{18} at 511 keV. Therefore, the degree of protection varies depending on the isotope in use and the corresponding photon energy levels [10]. The thickness values simulated in this study refer to lead-equivalent thicknesses, which are used to represent the radiation attenuation capacity of different protective eyewear materials. This standardization enables more accurate comparisons across shielding products regardless of their composition or actual physical thickness.

For glasses with a thickness of 0.75 mm, the protection efficiency was 11% for F^{18} radiation and 18% for I^{131} radiation. These values suggest minimal shielding effectiveness for these radionuclides. However, a significant improvement in protection was noted for Tc^{99m} radiation, where the efficiency exceeded 85%. It demonstrates that lead glasses provide substantial shielding against Tc^{99m} but are less effective for other radionuclides tested.

These findings highlight the importance of selecting appropriate protective equipment based on the specific radionuclides encountered in clinical or laboratory settings to ensure optimal safety for nuclear medicine professionals. Further investigation into enhancing the protective properties of lead glasses may be warranted to address the limitations observed for specific radionuclides.

To evaluate the effectiveness of lead glasses, a protection efficiency exceeding 50% was considered clinically beneficial based on prior shielding benchmarks in diagnostic imaging. This threshold aligns with the As Low As Reasonably Achievable (ALARA) principle, which emphasizes minimizing radiation exposure while balancing the practicality and comfort of protective measures. Although lead glasses provide significant dose reduction for

Table 3
The ratio of cornea-to-lens dose for all types of radiation examined in this study

	Radiation				
Eye glass (mm)	F^{18}	I^{131}	Tc^{99m}	X-ray 50 keV	X-ray 30 keV
0.0	1.104	1.094	1.187	3.81	6.80
0.05	1.107	1.098	1.191	1.60	2.72
0.07	1.105	1.097	1.191	-	-
0.10	1.106	1.097	1.195	1.47	1.93
0.20	1.105	1.099	1.199	1.44	1.70
0.30	1.108	1.097	1.200		
0.40	1.109	1.102	1.206		
0.50	1.116	1.102	1.208		
0.60	1.115	1.105	1.216		
0.70	1.116	1.108	1.220		
0.75	1.114	1.108	1.223		

Figure 2
Protection efficiency of lead eyeglasses with varying lead-equivalent thicknesses for different radionuclides

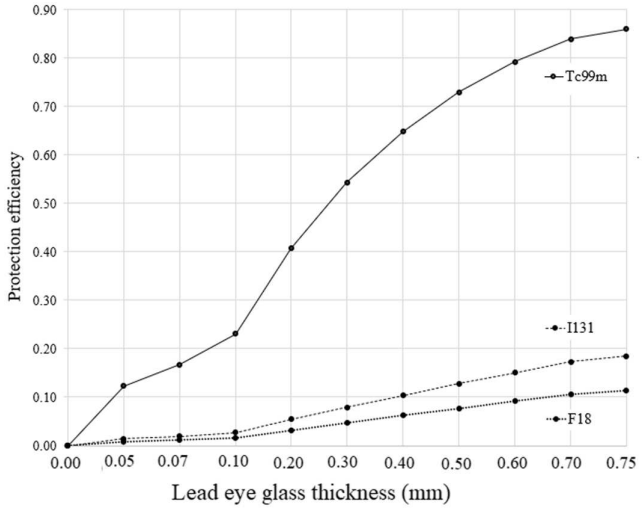

low-energy photons such as Tc-99m, they offer limited protection for high-energy emissions like F-18. Additionally, potential drawbacks such as discomfort, reduced visibility, and user compliance should be considered when weighing the cost-benefit of wearing such equipment in clinical settings [15].

Monte Carlo simulations using the Livermore physics model were conducted to evaluate dose reduction to the eye under different shielding conditions. Error bars in Figure 2 represent statistical uncertainties, all maintained below 1%, which may not be visible due to their small magnitude. The results confirm that this type of lead glass provides considerable efficiency for Tc-99m radiation; however, it offers limited protection against higher-energy emissions such as F-18 and I-131.

4. Discussion

Recent studies have increasingly focused on occupational eye dosimetry due to updated radiation protection guidelines and the recognized risk of cataract formation from low-dose exposures. Our findings contribute to this ongoing effort by evaluating the effectiveness of lead eyewear in reducing radiation dose to the eye.

These findings underscore the importance of evaluating protective eyewear's effectiveness in occupational settings, ensuring compliance with evolving safety standards while mitigating risks of radiation-induced ocular damage.

An experimental study conducted among nuclear medicine staff [9] utilized dosimetric measurements in Positron Emission Tomography (PET) settings and demonstrated that tasks such as FDG syringe preparation and radiotracer injection contribute the most to occupational eye lens dose, whereas other routine activities account for only a small proportion of cumulative exposure.

Further research has highlighted discrepancies between experimental studies and computational simulations. Hirakawa et al. [22] measured occupational eye lens doses using a direct Hp(3) eye dosimeter (DOSIRIS™) during interventional radiology procedures, providing experimental evidence that supports and complements simulation-based findings. In contrast, comparative analyses such as those reported by Hoeijmakers et al. [13] demonstrate that experimental measurements can differ from Monte Carlo estimates under certain conditions. This discrepancy is often attributed to the use of simplified geometries and low-resolution phantoms in simulations, as noted by Morhrasi et al. [2]. In our study, a high-resolution voxel phantom was employed, which offers a more anatomically accurate representation and contributes to more precise dose estimations. Overall, these comparisons reinforce the importance of phantom resolution in dose assessment and support the reliability of our simulation approach.

These findings indicate the need for advanced simulation techniques to enhance dose estimation accuracy, thereby improving radiation safety protocols for healthcare professionals in PET centers.

McCann et al. [11] further explored eye dosimetry using the EGSnrc Monte Carlo code through experimental and simulation methods. They assessed dose rates from unshielded and shielded syringes containing ^{68}Ga and ^{18}F, reporting approximately threefold higher doses for ^{68}Ga than ^{18}F, though no absolute values were provided.

Our study demonstrated doses of 8.21 μGy/MBq for F^{18}, 1.75 μGy/MBq for Tc^{99m}, and 5.69 μGy/MBq for I^{131}, which align well with previous empirical studies and corroborate their findings [11]. Here, MBq refers to one megabecquerel for a duration of one second (MBq·s), corresponding to one million disintegrations, which was used for dose normalization in the simulation. Although F^{18} exhibited the highest dose per unit activity, the larger activities

typically administered for I^{131} treatments in clinical practice may result in higher total exposure to technologists from I^{131} overall. In this simulation, dose values were calculated per megabecquerel (MBq) for a fixed geometry, assuming a standard source-to-eye distance and a constant exposure duration. This normalization allowed for direct comparison between radionuclides independent of clinical variations in time or positioning. While time and distance are critical in real-world settings, our approach focuses on the relative dose potential per unit activity. Actual occupational exposure would further depend on factors such as procedure duration, shielding practices, and handling frequency, which were not simulated here but are acknowledged as influential.

In Table 2, the radiation doses to various parts of the eye are presented. The data indicate that F^{18} delivers a significantly higher dose than other radionuclides. Specifically, the dose from F^{18} was observed to be 1.44 times higher than I^{131} and 4.6 times higher than Tc^{99m}. Analysis of the cumulative data for all radionuclides revealed no statistically significant differences between the lens dose and the total eye dose. This finding supports the conclusion that the lens dose can serve as a reliable representation of the total eye dose, which is crucial for ensuring the safety of radiation workers.

Conversely, significant differences were observed between the corneal and total eye doses. Notably, the corneal dose was approximately 10% higher than the lens dose for F^{18} and I^{131}, while for Tc^{99m}, this difference increased to approximately 19% (as shown in Table 3). These findings reveal the need to carefully consider corneal exposure in radiation protection protocols, mainly when using radionuclides with higher relative corneal doses.

The relationship between the cornea-to-lens dose ratio and the thickness of lead glasses reveals notable trends. As the thickness of lead glasses increases, the absorbed dose to both the cornea and lens decreases. However, the cornea-to-lens dose ratio rises with increasing eye shield thickness, indicating greater shielding effectiveness for the lens than the cornea. Specifically, the lens demonstrates enhanced protection with effectiveness increments of 0.010, 0.014, and 0.036 for F^{18}, I^{131}, and Tc^{99m}, respectively.

This phenomenon may be attributed to the sequential passage of radiation, which first traverses the cornea before reaching the lens. Additionally, electrons generated near the corneal surface contribute to this disparity. For instance, as shown in Table 3, 30 keV electrons impart significantly higher doses to the cornea than 50 keV. Furthermore, bremsstrahlung radiation produced by lead shielding can amplify this effect.

While lead glasses mitigate overall radiation exposure, their impact on dose distribution requires careful consideration. These findings highlight the need for optimized shielding designs to effectively balance protection for both ocular components.

In clinical practice, ceiling-suspended shields or bench-mounted lead glass barriers are frequently employed during the preparation and administration of radiopharmaceuticals. These fixed shielding devices are particularly useful for high-energy radionuclides such as F-18, providing effective eye dose reduction while improving comfort and user compliance compared to lead eyewear. Their integration into routine workflows offers a practical alternative or complement to personal protective equipment, especially in procedures involving prolonged exposure or repeated handling of radioactive materials [15].

Moreover, the increasing adoption of automated injectors in PET facilities has helped minimize direct handling of radiotracers, leading to significant reductions in extremity and eye doses for technologists [9]. These systems automate the syringe preparation and injection process, thus increasing operational safety and efficiency.

Based on this analysis, standard protective eyewear does not provide adequate protection against F^{18} and I^{131} radiation exposure. Consequently, leaded glass materials are strongly recommended to enhance ocular safety for personnel working with these specific radionuclides. It calls attention to the need for tailored protective measures in radiation safety protocols to address varying exposure risk levels associated with radionuclides.

5. Conclusion

Our study revealed that the absorbed dose to the cornea consistently exceeded that to the lens across all radionuclides evaluated. While this highlights the importance of including corneal dosimetry—alongside lens dosimetry—for a comprehensive assessment of ocular radiation exposure, it is important to note that the corneal dose levels observed in typical occupational settings are unlikely to cause biological harm. However, corneal dose tracking may still be useful in the context of prolonged exposure, shielding optimization, and safety protocol development.

While lead glasses reduce overall radiation exposure, they may increase the cornea-to-lens dose ratio, indicating unequal shielding effectiveness. F^{18} and I^{131} in particular demonstrated low shielding efficiency, whereas Tc^{99m} showed considerable dose reduction. These results point to a critical need for radionuclide-specific shielding strategies.

Ultimately, our findings advocate for tailored eye protection, especially in high-risk scenarios involving F^{18} or I^{131}, and call for further innovation in the design of shielding devices. Incorporating both lens and cornea protection will be essential in optimizing safety standards for nuclear medicine personnel.

Moreover, while leaded eyewear provides a measurable reduction in eye dose, particularly for low-energy photons, its design and comfort can influence user compliance in clinical environments. In scenarios involving high-energy radionuclides, where dose reduction from lead glasses is modest, ensuring proper workflow efficiency is important to avoid unnecessary exposure due to prolonged handling time.

According to ICRP recommendations [4], the annual equivalent dose limit of 150 mSv applies specifically to the lens of the eye for radiation workers, whereas the whole-body effective dose limit is 20 mSv. Clarifying this distinction is critical when evaluating occupational radiation protection.

Thus, optimal personal protective equipment (PPE) design must balance protective benefits with ergonomic efficiency to ensure overall dose reduction.

Acknowledgment

A pre-publication version of this manuscript was previously posted on the arXiv [23].

Ethical Statement

This study does not contain any studies with human or animal subjects performed by any of the authors.

Conflicts of Interest

The authors declare that they have no conflicts of interest to this work.

Data Availability Statement

Data sharing is not applicable to this article as no new data were created or analyzed in this study.

Author Contribution Statement

Zahra Akbari Khanaposhtani: Conceptualization, Methodology, Software, Formal analysis, Investigation, Data curation, Writing – original draft, Visualization. **Hossein Rajabi:** Conceptualization, Methodology, Validation, Resources, Writing – review & editing, Supervision, Project administration.

References

[1] Kollaard, R., Zorz, A., Dabin, J., Covens, P., Cooke, J., Crabbé, M., . . . , & McNamara, L. (2021). Review of extremity dosimetry in nuclear medicine. *Journal of Radiological Protection*, *41*(4), R60–R87. https://doi.org/10.1088/1361-6498/ac31a2

[2] Morhrasi, P., Jumpee, C., Charoenphun, P., & Chuamsaamarkkee, K. (2022). Estimation of occupational eye lens dose in nuclear medicine: A Monte Carlo study. *Journal of Medical Imaging and Radiation Sciences*, *53*(4), S29. https://doi.org/10.1016/j.jmir.2022.10.095

[3] Hamada, N., Azizova, T. V., & Little, M. P. (2020). An update on effects of ionizing radiation exposure on the eye. *The British Journal of Radiology*, *93*(1115), 20190829. https://doi.org/10.1259/bjr.20190829

[4] Stewart, F. A., Akleyev, A. V., Hauer-Jensen, M., Hendry, J. H., Kleiman, N. J., MacVittie, T. J., . . . , & Wallace, W. H. (2012). ICRP publication 118: ICRP statement on tissue reactions and early and late effects of radiation in normal tissues and organs — Threshold doses for tissue reactions in a radiation protection context. *Annals of the ICRP*, *41*(1-2), 1–322. https://doi.org/10.1016/j.icrp.2012.02.001

[5] Hamada, N. (2017). Ionizing radiation sensitivity of the ocular lens and its dose rate dependence. *International Journal of Radiation Biology*, *93*(10), 1024–1034. https://doi.org/10.1080/09553002.2016.1266407

[6] Chen, X., Xu, J., Chen, X., & Yao, K. (2021). Cataract: Advances in surgery and whether surgery remains the only treatment in future. *Advances in Ophthalmology Practice and Research*, *1*(1), 100008. https://doi.org/10.1016/j.aopr.2021.100008

[7] Volatier, T., Schumacher, B., Cursiefen, C., & Notara, M. (2022). UV protection in the cornea: Failure and rescue. *Biology*, *11*(2), 278. https://doi.org/10.3390/biology11020278

[8] Bellamy, M. B., Miodownik, D., Quinn, B., & Dauer, L. (2020). Occupational eye lens dose over six years in the staff of a US high-volume cancer center. *Radiation Protection Dosimetry*, *192*(3), 321–327. https://doi.org/10.1093/rpd/ncaa187

[9] Fujisawa, M., Haga, Y., Sota, M., Abe, M., Kaga, Y., Inaba, Y., . . . , & Chida, K. (2023). Evaluation of lens doses among medical staff involved in nuclear medicine: Current eye radiation exposure among nuclear-medicine staff. *Applied Sciences*, *13*(16), 9182. https://doi.org/10.3390/app13169182

[10] Gangl, A., Deutschmann, H. A., Portugaller, R. H., & Stücklschweiger, G. (2022). Influence of safety glasses, body height and magnification on the occupational eye lens dose during pelvic vascular interventions: A phantom study. *European Radiology*, *32*(3), 1688–1696. https://doi.org/10.1007/s00330-021-08231-y

[11] McCann, A., Cournane, S., Dowling, A., Maguire, D., Lucey, J., & Leon, L. (2021). Assessment of operator exposure from shielded and unshielded sources of 18F and 68Ga–Monte Carlo simulations and empirical measurements. *Physica Medica: European Journal of Medical Physics*, *84*, 297–298. https://doi.org/10.1016/j.ejmp.2021.01.039

[12] Behrens, R., & Dietze, G. (2011). Dose conversion coefficients for photon exposure of the human eye lens. *Physics in Medicine & Biology*, *56*(2), 415–437. https://doi.org/10.1088/0031-9155/56/2/009

[13] Hoeijmakers, E. J., Hoenen, K., Bauwens, M., Eekers, D. B., Jeukens, C. R., & Wierts, R. (2024). Dose rate conversion coefficients for ocular contamination in nuclear medicine: A Monte Carlo simulation with experimental validation. *Medical Physics*, *51*(8), 5645–5653. https://doi.org/10.1002/mp.17073

[14] Nuzzi, R., Trossarello, M., Bartoncini, S., Marolo, P., Franco, P., Mantovani, C., & Ricardi, U. (2020). Ocular complications after radiation therapy: An observational study. *Clinical Ophthalmology*, *14*, 3153–3166. https://doi.org/10.2147/OPTH.S263291

[15] Akahane, M., Yoshioka, N., & Kiryu, S. (2022). Radiation protection of the eye lens in fluoroscopy-guided interventional procedures. *Interventional Radiology*, *7*(2), 44–48. https://doi.org/10.22575/interventionalradiology.2022-0006

[16] Hirata, Y., Fujibuchi, T., Fujita, K., Igarashi, T., Nishimaru, E., Horita, S., . . . , & Ono, K. (2019). Angular dependence of shielding effect of radiation protective eyewear for radiation protection of crystalline lens. *Radiological Physics and Technology*, *12*(4), 401–408. https://doi.org/10.1007/s12194-019-00538-2

[17] Strulab, D., Santin, G., Lazaro, D., Breton, V., & Morel, C. (2003). GATE (Geant4 application for tomographic emission): A PET/SPECT general-purpose simulation platform. *Nuclear Physics B-Proceedings Supplements*, *125*, 75–79. https://doi.org/10.1016/S0920-5632(03)90969-8

[18] Agostinelli, S., Allison, J., Amako, K., Apostolakis, J., Araujo, H., Arce, P., . . . , & Zschiesche, D. (2003). Geant4—A simulation toolkit. *Nuclear Instruments and Methods in Physics Research Section A: Accelerators, Spectrometers, Detectors and Associated Equipment*, *506*(3), 250–303. https://doi.org/10.1016/S0168-9002(03)01368-8

[19] Mello, G. R., Rocha, K. M., Santhiago, M. R., Smadja, D., & Krueger, R. R. (2012). Applications of wavefront technology. *Journal of Cataract & Refractive Surgery*, *38*(9), 1671–1683. https://doi.org/10.1016/j.jcrs.2012.07.004

[20] O'Donoghue, J., Zanzonico, P., Humm, J., & Kesner, A. (2022). Dosimetry in radiopharmaceutical therapy. *Journal of Nuclear Medicine*, *63*(10), 1467–1474. https://doi.org/10.2967/jnumed.121.262305

[21] Boone, J. M., & Seibert, J. A. (1997). An accurate method for computer-generating tungsten anode x-ray spectra from 30 to 140 kV. *Medical Physics*, *24*(11), 1661–1670. https://doi.org/10.1118/1.597953

[22] Hirakawa, M., Nakatake, H., Tsuruta, S., Matsuura, S., Motomura, Y., Hiraki, Y., . . . , & Ishigami, K. (2022). Dosimetry of occupational eye lens dose using a novel direct eye dosimeter, DOSIRIS, during interventional radiology procedures. *Interventional Radiology*, *7*(2), 40–43. https://doi.org/10.22575/interventionalradiology.2022-0005

[23] Khanaposhtani, Z. A., & Rajabi, H. (2025). *Comparative analysis of corneal and lens doses in nuclear medicine and impact of lead eyeglasses: A Monte Carlo simulation approach*, *arXiv Preprint: 2508.19370*.

How to Cite: Khanaposhtani, Z. A., & Rajabi, H. (2026). Comparative Analysis of Corneal and Lens Doses in Nuclear Medicine and Impact of Lead Eyeglasses: A Monte Carlo Simulation Approach. *Journal of Optics and Photonics Research*. https://doi.org/10.47852/bonviewJOPR62025710